

# Evaluation of $^{18}\text{F}$ -FDG Uptake and Arterial Wall Calcifications Using $^{18}\text{F}$ -FDG PET/CT

Simona Ben-Haim, MD, DSc<sup>1,2</sup>; Ela Kupzov, PhM<sup>3</sup>; Ada Tamir, DSc<sup>2,4</sup>; and Ora Israel, MD<sup>2,3</sup>

<sup>1</sup>Department of Nuclear Medicine, Carmel Medical Center, Haifa, Israel; <sup>2</sup>The B. Rapaport Faculty of Medicine, Technion, Israel Institute of Technology, Haifa, Israel; <sup>3</sup>Department of Nuclear Medicine, Rambam Medical Center, Haifa, Israel; and <sup>4</sup>Department of Epidemiology and Biostatistics, Carmel Medical Center, Haifa, Israel

Glucose metabolic activity expressed as  $^{18}\text{F}$ -FDG uptake may be increased in active atherosclerotic plaque. Calcium depositions are often increased in mature atherosclerotic plaque. The purpose of the present study was to assess the patterns of vascular-wall  $^{18}\text{F}$ -FDG uptake and CT calcifications using combined PET/CT. **Methods:** One hundred twenty-two consecutive patients over the age of 50 (47 women and 75 men; mean age,  $66 \pm 9$  y) undergoing whole-body  $^{18}\text{F}$ -FDG PET/CT for tumor assessment were retrospectively evaluated. PET, CT, and PET/CT slices were generated for review. Abnormal vascular findings in major arteries in the chest and abdomen were categorized as PET positive (PET+), PET negative (PET-), CT positive (CT+), or CT negative (CT-). The topographic relationship between increased vascular-wall  $^{18}\text{F}$ -FDG uptake on PET and the presence of calcifications on CT was assessed on PET/CT fused images, with abnormal sites further classified as PET+/CT+, PET+/CT-, or PET-/CT+. The presence of CT calcifications and increased vascular-wall  $^{18}\text{F}$ -FDG uptake was correlated with age, sex, presence of cardiovascular risk factors, and cardiovascular disease. **Results:** Abnormal findings were identified at 349 sites. CT calcifications (CT+) were observed at 320 sites (92%) of 100 patients (82%), more commonly in men ( $P < 0.03$ ), in older patients ( $P < 0.0001$ ), in patients with hypertension ( $P < 0.003$ ) or hyperlipidemia ( $P < 0.04$ ), and in smokers ( $P < 0.008$ ). Increased vascular-wall  $^{18}\text{F}$ -FDG uptake (PET+) was observed at 52 sites (15%) of 38 patients (31%), more commonly in men ( $P < 0.02$ ), in older patients ( $P < 0.0001$ ), and in patients with hypertension ( $P < 0.02$ ), and was borderline in patients with cardiovascular disease ( $P = 0.057$ ). PET+ and CT+ findings correlated in 12 patients, a PET+/CT- pattern was found in 18 patients, and 8 patients had increased vascular-wall  $^{18}\text{F}$ -FDG uptake in sites with and without calcifications (PET+/CT+, CT-). Twenty-two patients (18%) had a PET-/CT- pattern. **Conclusion:** Hybrid PET/CT can be used to identify and to correctly localize vascular-wall  $^{18}\text{F}$ -FDG activity. Increased vascular-wall  $^{18}\text{F}$ -FDG activity was found in 15% of sites and CT calcifications were noted in 92% of sites, with congruent findings in 7%. The clinical significance of the relationship between vascular-wall  $^{18}\text{F}$ -FDG

uptake and CT calcifications needs to be assessed by further prospective studies with long-term follow up.

**Key Words:** hybrid imaging; PET/CT; atherosclerosis; arterial calcifications

**J Nucl Med 2004; 45:1816-1821**

Atherosclerosis is one of the leading causes of morbidity and mortality in the world. Yet, if identified early, atherosclerosis can be treated with dietary and lifestyle changes and with medications. The fine structure and composition of the atherosclerotic lesion, rather than the degree of stenosis, are currently considered to be the important determinants for acute clinical events, together with the absence of collateral circulation (1).

Most techniques for visualization and characterization of the atherosclerotic plaque, such as intravascular ultrasound or angiography, are catheter based. They reveal, as a rule, only single atherosclerotic plaques at the local level (1-5). Atherosclerosis can also be diagnosed from imaging modalities that offer either excellent anatomic resolution of the arterial lumen (angiography and magnetic resonance angiography) or detection of calcium in the arterial wall (electron beam CT and multidetector CT) (6-10). Angiography suffers from significant interobserver variability (6). Magnetic resonance angiography may overestimate disease extent, conventional CT with long acquisition times is not a reliable screening tool, and the role of multidetector CT in the detection and serial monitoring of coronary artery calcifications has yet to be determined. These anatomic imaging modalities reveal the arterial lumen or calcifications, which are believed to represent late events in the atherosclerotic process.

An imaging modality that can detect and localize inflammatory changes in the arterial wall, representing early stages of atherosclerosis, is presently lacking. Radiotracers, such as  $^{99\text{m}}\text{Tc}$ -radiolabeled low-density lipoprotein, have been reported to accumulate in atherosclerotic plaques, whereas  $^{111}\text{In}$ - or  $^{99\text{m}}\text{Tc}$ -labeled antibodies against plaque, fibrin, and its degradation products or platelets have been used for

Received Feb. 8, 2004; revision accepted May 24, 2004.

For correspondence or reprints contact: Simona Ben-Haim, MD, DSc, Department of Nuclear Medicine, Carmel Medical Center, 7, Michal St., Haifa, 34362, Israel.

E-mail: simona\_ben-haim@clalit.org.il

targeting the cells or molecules involved in atherosclerotic lesions in an experimental setting (11–13). Most agents have, however, unfavorable diagnostic properties such as slow blood clearance, low target-to-background ratio, or an affinity to nonspecific binding sites.

$^{18}\text{F}$ -FDG PET is routinely used in the evaluation of cancer. However,  $^{18}\text{F}$ -FDG is a nonspecific tracer and accumulates also in sites of infection and inflammation. Increased vascular-wall  $^{18}\text{F}$ -FDG uptake in the large blood vessels has been noted in 60% of patients older than 60 y (14–17). PET is limited by its inability to precisely localize the site of increased tracer uptake. Correlation of PET findings with anatomic imaging modalities, such as CT or MRI, is therefore often required, but precise alignment of images can be difficult (18).

A novel technology of combined PET and CT acquisition using the same imaging device has recently been introduced, allowing for correct fusion of images of both modalities obtained sequentially in a single session (17,18).

The purpose of the present study was to assess the imaging patterns of vascular-wall  $^{18}\text{F}$ -FDG uptake and CT calcifications in the wall of large arteries using the new technology of hybrid PET/CT.

## MATERIALS AND METHODS

### Patient Population

One hundred and 22 consecutive cancer patients 50 y or older and undergoing clinical tumor  $^{18}\text{F}$ -FDG PET/CT studies were retrospectively enrolled in the study. A detailed clinical history on the presence of cardiovascular risk factors such as diabetes, obesity, smoking, hypertension, and hyperlipidemia and a history of cardiovascular disease or cardiovascular events (myocardial infarction or cerebrovascular accident) was obtained for all patients. The histologic tumor type and history of previous chemotherapy or radiotherapy were also recorded. There were 47 female patients and 75 male patients, with an average age of  $66 \pm 9$  y. The clinical characteristics of the patients are summarized in Table 1. The study was approved by the Institutional Review Board.

### Imaging Technique

All studies were performed according to the routine protocol using a dedicated PET/CT system (Discovery LS; General Electric Medical Systems). This device comprises a dedicated PET scanner with a full-ring bismuth germanate detector and a multislice CT scanner (17). The PET and CT components are mounted back-to-back and mechanically calibrated to ensure alignment of the CT and PET planes to within 2 mm over the transaxial field of view. The imaging protocol consisted of an initial CT acquisition followed by the PET study. The CT acquisition parameters included 140 kV, 80 mA, 4 helical slices, 0.5 s/rotation, a pitch of 6:1 covering 1 m, and a slice thickness of 5 mm. The PET images were of sequential 15-cm fields of view and were acquired over 5 min in 2-dimensional mode using a matrix of  $128 \times 128$ , followed by reconstruction using ordered-subsets expectation maximization. CT images were reconstructed onto a  $512 \times 512$  matrix, and these data, expressed as Hounsfield units, were converted into 511-keV-equivalent attenuation factors for attenuation correction. Matching

**TABLE 1**  
Patients' Clinical Characteristics

Characteristic	Value
Total patient population	122
Sex (male)	75 (61%)
Age (y)	Mean $\pm$ SD, $66 \pm 9$ ; range, 51–84
Clinical history	
Diabetes	28 (23%)
Hypertension	46 (38%)
Hyperlipidemia	34 (28%)
Obesity	20 (16%)
Smoking	66 (54%)
Cardiovascular history	18* (15%)
Tumors	
Lung	41 (34%)
Lymphoma	34 (28%)
Colon	21 (17%)
Breast	8 (7%)
Melanoma	4 (3%)
Others	24 (20%)
Previous treatment	
Chemotherapy	44 (36%)
Radiotherapy	10 (8%)
Chemo- and radiotherapy	22 (18%)

\*Includes 12 patients with myocardial infarction, 6 with cerebrovascular accident, and 10 with revascularization.

PET and CT slices were fused, and an image of the  $^{18}\text{F}$ -FDG activity overlying the corresponding anatomic plane was generated using a dedicated workstation (Entegra or Xeleris; General Electric Medical Systems).

Patients fasted for 4–6 h before injection of  $^{18}\text{F}$ -FDG except for glucose-free oral hydration. Blood glucose was measured before injection of the tracer. Blood glucose levels were  $108 \pm 13$  mg/dL (range, 85–143 mg/dL) in nondiabetic patients and  $163 \pm 79$  mg/dL (range, 83–382 mg/dL) in diabetic patients. The injected dose of  $^{18}\text{F}$ -FDG was 370–555 MBq (10–15 mCi). After injection, patients kept lying comfortably. The urinary bladder was not catheterized. Oral muscle relaxants were not administered. PET/CT was started 60 min after  $^{18}\text{F}$ -FDG injection. No oral or intravenous contrast material was administered for the CT.

### Image Interpretation

CT, PET, and fused PET/CT images were generated for review. CT images were evaluated visually for sites of abnormal vascular calcifications, defined as high-density mural areas. Both uncorrected and attenuation-corrected PET images were evaluated visually for focal areas of abnormal  $^{18}\text{F}$ -FDG uptake. Linear and diffuse patterns of increased  $^{18}\text{F}$ -FDG uptake, previously described in patients with arteritis (19,20), were not included for further evaluation in this study. The location of focal  $^{18}\text{F}$ -FDG uptake in relation to the vascular wall and to CT calcifications was determined using the corresponding fused PET/CT slices. PET/CT images were also evaluated for the presence of respiratory motion artifacts and of misregistration between the PET and CT components. Based on the separate PET and CT findings for the vascular wall, the lesions were categorized as PET positive (PET+), PET negative (PET–), CT positive (CT+), or CT negative (CT–).

Based on the fused-image findings, the sites were further classified as PET+/CT+, PET+/CT−, or PET−/CT+. The same categories were used for the patient-based analysis. In addition, patients showing no vascular-wall abnormalities on PET or CT were defined as PET−/CT−. The number of patients with multiple lesions was also recorded.

## Data Analysis

Statistical Package for Social Sciences (version 11.0; SPSS Inc.) was used for statistical analysis. The prevalence of calcifications on CT and increased vascular-wall <sup>18</sup>F-FDG uptake on PET was calculated. The relationship between the presence and location of <sup>18</sup>F-FDG uptake and CT calcifications, and the association of these findings and the patients' clinical characteristics, were evaluated. Data are reported as mean ± SD. Groups were compared using the *t* test for continuous variables and the  $\chi^2$  test for categorical variables. A *P* value of less than 0.05 was considered statistically significant.

## RESULTS

Increased <sup>18</sup>F-FDG uptake in the vascular wall and CT calcifications were found at 349 sites in 100 of the 122 patients in the study.

### Site-Based Analysis

CT calcifications were observed at 320 sites (92%) in 100 patients (82%). At 135 sites (39% of all sites; 42% of CT+ sites), calcifications were noted in the thoracic aorta; at 174 sites (50% of all sites; 54% of CT+ sites), in the abdominal arteries; and at 11 sites (3% of all sites; 3% of CT+ sites), in the carotid arteries (Table 2). Increased vascular-wall <sup>18</sup>F-FDG uptake was observed at 52 sites (15%) in 38 patients. At 31 sites (9% of all sites; 60% of PET+ sites), uptake was noted in the thoracic aorta; at 20 sites (6% of all sites; 60% of PET+ sites), in abdominal arteries; and at 1 site (0.2% of all sites; 2% of PET+ sites), in the carotid artery (Table 2). All sites of <sup>18</sup>F-FDG uptake were seen both on uncorrected and on CT-based attenuation-corrected PET images. No areas of respiratory motion artifacts or misregistration were observed.

Of the 349 sites in total, 23 (7%) were PET+/CT+, 29 (8%) were PET+/CT−, and 297 (85%) were PET−/CT+. The distribution of lesions and their patterns, and their

localization in the different great vessels, are presented in Table 2.

### Patient-Based Analysis

Vascular CT wall calcifications were demonstrated in 100 patients (82%). Seventy-six patients showed multiple sites of calcifications on CT (range, 2–9 calcifications per patient). The group of patients showing CT calcifications included significantly more men than women (88% of the men vs. 72% of the women, *P* < 0.03), older patients (mean age of 68 ± 8.3 y for patients who showed CT calcifications vs. 57 ± 7.4 y for those who did not, *P* < 0.0001), patients with hypertension (96% with hypertension vs. 74% without, *P* < 0.003), patients with hyperlipidemia (94% with hyperlipidemia vs. 78% without, *P* < 0.04), smokers (93% smokers vs. 70% patients with no smoking history, *P* < 0.008), and patients with known cardiovascular disease (100% of patients with known cardiovascular disease vs. 78% of patients without, *P* < 0.02).

Increased vascular-wall <sup>18</sup>F-FDG uptake was observed in 38 patients (31%). Thirteen patients showed more than one site of increased <sup>18</sup>F-FDG uptake on PET (range, 2–3 sites per patient). The group of patients with abnormal vascular-wall <sup>18</sup>F-FDG uptake included significantly more men than women (37% of the men vs. 17% of the women, *P* < 0.02), older patients (mean age of 71 ± 7 y for patients who showed abnormal uptake vs. 64 ± 9 y for those who did not, *P* < 0.0001), and patients with hypertension (42% with hypertension vs. 22% without, *P* < 0.02) and, at borderline significance, included more patients with known cardiovascular disease (47% of patients with known cardiovascular disease vs. 26% of patients without, *P* = 0.057).

No statistically significant correlation was found between the presence of vascular-wall <sup>18</sup>F-FDG uptake or CT calcifications and prior chemotherapy or radiotherapy.

Of the 38 patients with increased vascular-wall <sup>18</sup>F-FDG uptake, PET abnormalities correlated with CT calcifications (PET+/CT+) (Fig. 1) in 12 patients (10% of all, 32% of PET+). Eighteen patients (15% of all, 47% of PET+) had abnormal <sup>18</sup>F-FDG localization in areas with no corresponding calcifications (PET+/CT−) (Fig. 2), and in 8 patients (7% of all, 21% of PET+), increased vascular-wall <sup>18</sup>F-FDG uptake was noted in sites with and in other sites without calcifications on CT (PET+/CT+, CT−). Sixty-two patients (51%) showed only CT calcifications and were classified as PET−/CT+. No statistically significant differences were found when the clinical characteristics of the patients in each of these groups were compared with those of the total study population.

Twenty-two patients (18%) showed no vascular-wall lesions on either PET or CT and were defined as PET−/CT−. Compared with the total study population, these patients were significantly younger (58.6 ± 7.4 y vs. 65.8 ± 8.9 y, *P* < 0.0001) and were less likely to have hypertension (10%

**TABLE 2**  
Distribution of CT Calcifications and Vascular Wall <sup>18</sup>F-FDG Uptake

Site	Number of sites			Total
	PET+/CT+	PET+/CT−	PET−/CT+	
Thoracic aorta	12 (3%)	19 (5%)	123 (35%)	154 (44%)
Abdominal arteries	10 (3%)	10 (3%)	164 (47%)	184 (53%)
Carotid arteries	1 (0%)	0 (0%)	10 (3%)	11 (3%)
Total	23 (7%)	29 (8%)	297 (85%)	349 (100%)



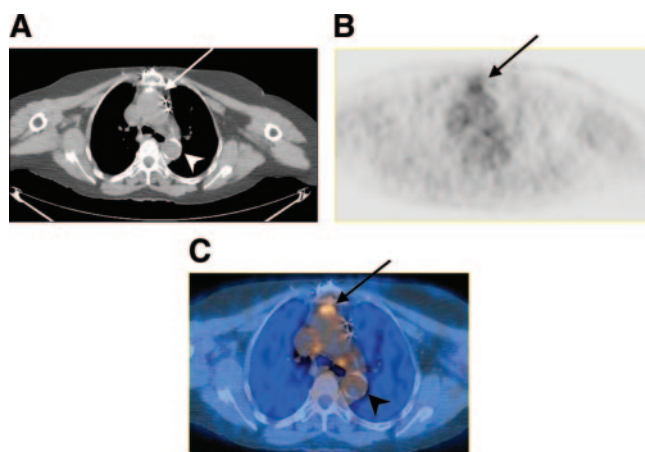


**FIGURE 1.** A 71-y-old woman with a history of breast carcinoma and colon cancer and a medical history of hypertension. CT (A),  $^{18}\text{F}$ -FDG PET (B), and fused PET/CT (C) images show CT calcifications in wall of thoracic aorta with (arrow) and without (arrowhead) focal  $^{18}\text{F}$ -FDG uptake.

vs. 38%,  $P < 0.04$ ) or a history of smoking (24% vs. 55%,  $P < 0.04$ ).

Sixteen patients (13%) had a history of cardiovascular events including myocardial infarction ( $n = 12$ ), a cerebrovascular accident ( $n = 6$ ), or both events ( $n = 2$ ). CT calcifications were present in all 16 patients. Increased vascular-wall  $^{18}\text{F}$ -FDG uptake was present in 8 of these 16 patients (50%), compared with 38 patients (31%) with PET+ sites in the entire study population (Table 3).

## DISCUSSION

Atherosclerosis is one of the leading worldwide causes of death. More than 500,000 Americans die each year of coronary artery disease, and more than 90% of sudden deaths occur in individuals with 2 or more arteries narrowed

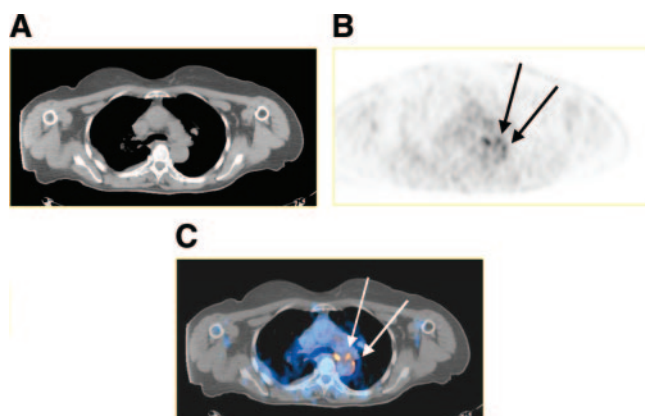


**FIGURE 2.** A 72-y-old man with colon carcinoma and known ischemic heart disease and who underwent coronary artery bypass grafting 13 y previously. CT (A),  $^{18}\text{F}$ -FDG PET (B), and fused PET/CT (C) images show focally increased  $^{18}\text{F}$ -FDG uptake in wall of thoracic aorta (arrows) with no corresponding CT calcification.

**TABLE 3**  
Number of Abnormal Sites: Comparison of Patients with History of Cardiovascular Events and Entire Patient Population

Imaging result	Patients with history of event*		Entire patient population	
	No. patients	No. sites	No. patients	No. sites
PET+/CT+	5	5	20	23
PET+/CT−	6	9	26	29
PET−/CT+	16	60	62	297
PET+/CT+ or CT−	8	14	38	52

\*Myocardial infarction or cerebrovascular accident.

by atherosclerosis. Yet, if identified early, atherosclerosis can be reversed by medications and dietary and lifestyle changes.

In a rabbit model of arterial wall injury, the amount of  $^{18}\text{F}$ -FDG uptake in atherosclerotic lesions correlated with the density of macrophages in the lesions (15). In a hypercholesterolemic rabbit model of atherosclerotic plaque, increased vascular-wall  $^{18}\text{F}$ -FDG uptake was shown to correspond to lesions with intimal proliferation and to correlate with a dense infiltrate of macrophages, vascular smooth muscle cells, and lymphocytes (21,22), suggesting increased  $^{18}\text{F}$ -FDG uptake as a possible indicator of vulnerable plaque.  $^{18}\text{F}$ -FDG uptake appears to be related to the size of plaques. Large plaques accumulate more  $^{18}\text{F}$ -FDG than do smaller or less bulky lesions. In addition, the amount of  $^{18}\text{F}$ -FDG uptake decreased significantly in animals whose diet was changed from high cholesterol to normal.

Diffusely increased  $^{18}\text{F}$ -FDG uptake along vascular walls in the large cervical and thoracic vessels has been described in patients with vasculitis (19,20,23).  $^{18}\text{F}$ -FDG uptake in vasculitis is nonspecific and may be related to smooth muscle proliferation or to the presence of macrophages within plaques (14,16,17,24). Vasculitis and atherosclerosis may show different patterns of  $^{18}\text{F}$ -FDG uptake. Diffuse and linear  $^{18}\text{F}$ -FDG activity along the arterial wall, rather than focally increased uptake, may be observed.

Hybrid PET/CT enables correct fusion of data obtained from the 2 modalities performed sequentially in a single session (17,18) and may therefore help to overcome false-positive results in oncology patients (25). It allows for an improved correlation between PET-expressed dynamic changes of function and metabolism on the one hand and the CT-expressed static state of anatomy and structure on the other hand.

Increased  $^{18}\text{F}$ -FDG uptake in the arterial wall in humans has been shown to become more frequent with advancing age (14,19,22). Yun et al. (14) demonstrated increased  $^{18}\text{F}$ -FDG uptake in the large arteries of 50% of cancer

patients 60 y and older and also found age and hypercholesterolemia to be the only parameters significantly correlating with vascular-wall  $^{18}\text{F}$ -FDG uptake (17). In a preliminary report on 8 patients with carotid atherosclerosis,  $^{18}\text{F}$ -FDG uptake was higher in symptomatic lesions than in the contralateral asymptomatic lesions (16). Tatsumi et al. (24) observed  $^{18}\text{F}$ -FDG uptake in the wall of the thoracic aorta in 59% of cancer patients, whereas large arteries below the diaphragm were not analyzed. In 16% of their patients this uptake was focal. The present study showed a relatively low incidence—31% of the patient population—of focal increased vascular-wall  $^{18}\text{F}$ -FDG uptake in the large arteries above and below the diaphragm.

CT calcifications in the thoracic aorta were found by Tatsumi et al. in 53% of patients, as opposed to the 83% of patients who showed CT calcifications in the thoracic aorta and large intraabdominal arteries in the present study. The 14% of patients showing  $^{18}\text{F}$ -FDG uptake in sites of calcifications in the study of Tatsumi et al. (24) is similar to the 16% found in the present study.

A few potential limitations may impair the data analysis of this study. CT attenuation correction or respiratory motion may create reconstruction artifacts leading to false-positive  $^{18}\text{F}$ -FDG uptake. No differences in findings were, however, observed in comparisons of attenuation-corrected and -uncorrected images. Other factors that may induce vascular-wall  $^{18}\text{F}$ -FDG uptake have to be considered. One such factor is vasculitis, but it was not reported in the clinical history of any patients in this study. Altered  $^{18}\text{F}$ -FDG uptake because of previous chemo- or radiotherapy may potentially lead to false-positive results, mainly in the presence of an incongruent PET+/CT− pattern. However, in the present study, no statistically significant differences were found between the incidences of the different PET/CT patterns before and after therapy.

Histopathologic results were not available in this retrospective study, and therefore no definite conclusions could be drawn about the clinical significance of the described PET/CT patterns. Because focal  $^{18}\text{F}$ -FDG uptake was not closely associated with CT calcifications, one may hypothesize that metabolic and morphologic imaging modalities provide different types of information on active or chronic lesions. The different and, at times, incongruent imaging patterns described in the present study may reflect a different anatomic and metabolic status in early or active versus late or inactive atherosclerotic plaques. Whether a correlation exists with plasma concentration of C-reactive protein, which expresses the intensity of occult plaque inflammation and the vulnerability to rupture, needs to be assessed. The hypothesis that some foci of increased vascular-wall  $^{18}\text{F}$ -FDG uptake may correspond to early atherosclerosis and may indicate the presence of a “vulnerable” plaque needs to be further tested by prospective studies assessing the prognostic value of  $^{18}\text{F}$ -FDG PET/CT patterns. If proven useful,  $^{18}\text{F}$ -FDG PET/CT may be the tool for early detection of

patients at increased risk of future cardiovascular events and for assessment of early therapies for vascular-wall lesions.

## CONCLUSION

Combined PET/CT can identify and localize focal vascular-wall  $^{18}\text{F}$ -FDG uptake. Three patterns of CT calcifications and  $^{18}\text{F}$ -FDG uptake in the vascular wall were noted in patients over the age of 50 y undergoing routine  $^{18}\text{F}$ -FDG PET/CT studies for evaluation of cancer. Increased  $^{18}\text{F}$ -FDG uptake was present in 6% of sites (16% of patients) with concomitant vascular calcifications observed on CT and in 7% of sites (21% of patients) with no corresponding structural findings. Further investigations are needed to assess the clinical significance and potential prognostic value of this modality as a tool for early diagnosis of “vulnerable” arterial plaques.

## ACKNOWLEDGMENTS

The authors thank Dr. J. Anthony Parker (Beth Israel Deaconess Medical Center) for his many useful suggestions on preparing the manuscript. This research was partly supported by an Eliyahu Pen Technion research grant.

## REFERENCES

1. Pasterkamp G, Falk E, Woutman H, Borst C. Techniques characterizing the coronary atherosclerotic plaque: influence on clinical decision making? *J Am Coll Cardiol*. 2000;36:13–21.
2. Gussenhoven EJ, Essed CE, Lancee CT, et al. Arterial wall characteristics determined by intravascular ultrasound imaging: an in vitro study. *J Am Coll Cardiol*. 1989;14:947–952.
3. Peters RJG, Kok WEM, Havenith MG, Rijsterborgh H, van der Wal AC, Visser CA. Histopathologic validation of intracoronary ultrasound imaging. *J Am Soc Echocardiography*. 1994;7:230–241.
4. Siegel RJ, Ariani M, Fishbein MC, et al. Histopathologic validation of angiography and intravascular ultrasound. *Circulation*. 1991;84:109–117.
5. Stefanadis C, Diamantopoulos L, Vlachopoulos C, et al. Thermal heterogeneity within human atherosclerotic coronary arteries detected in vivo. *Circulation*. 1999;99:1965–1971.
6. Galbraith J, Murphy M, de Soyza N. Coronary angiogram interpretation: inter-observer variability. *JAMA*. 1978;240:2053–2056.
7. Raggi P. Coronary calcium on electron beam tomography imaging as a surrogate marker of coronary artery disease. *Am J Cardiol*. 2001;87:27A–34A.
8. Toussaint J, LaMuraglia G, Southern J, et al. Magnetic resonance images lipid, fibrous, calcified, hemorrhagic, and thrombotic components of human atherosclerosis in vivo. *Circulation*. 1996;94:932–938.
9. Helft G, Worthley S, Fuster V, et al. Atherosclerotic aortic component quantification by noninvasive magnetic resonance imaging: an in vivo study in rabbits. *J Am Coll Cardiol*. 2001;37:1149–1154.
10. Moser KW, O'Keefe JH, Bateman TM, McGhie IA. Coronary calcium screening in asymptomatic patients as a guide to risk factor modification and stress myocardial perfusion imaging. *J Nucl Cardiol*. 2003;10:590–598.
11. Vallabhajosula S, Paidi M, Badimon JJ, et al. Radiotracers for low density lipoprotein biodistribution studies in vivo: technetium-99m preparations. *J Nucl Med*. 1988;29:1237–1245.
12. Fishman AJ, Rubin RH, Khaw BA, et al. Radionuclide imaging of experimental atherosclerosis with non-specific polyclonal immunoglobulin G. *J Nucl Med*. 1989;30:1095–1100.
13. Demacker PNM, Dormans TPJ, Koenders EB, Corstens FHM. Evaluation of Indium-111-polyclonal immunoglobulin G to quantitate atherosclerosis in Watanabe heritable hyperlipidemic rabbits with scintigraphy: effect of age and treatment with antioxidants or ethinylestradiol. *J Nucl Med*. 1993;34:1316–1321.
14. Yun M, Yeh D, Araujo LI, Jang S, Newberg A, Alavi A. F-18 FDG uptake in the large arteries, a new observation. *Clin Nucl Med*. 2001;26:314–319.
15. Lederman RJ, Raylman RR, Fisher SJ, et al. Detection of atherosclerosis using a

- novel positron-sensitive probe and 18-fluorodeoxyglucose (FDG). *Nucl Med Commun.* 2001;22:747–753.
16. Rudd JH, Warburton EA, Fryer TD, et al. Imaging atherosclerotic plaque inflammation with [ $^{18}\text{F}$ ]-fluorodeoxyglucose positron emission tomography. *Circulation.* 2002;105:2708–2711.
  17. Yun M, Jang S, Cucciara A, Newberg AB, Alavi A.  $^{18}\text{F}$ FDG uptake in the large arteries: a correlation study with the atherogenic risk factors. *Semin Nucl Med.* 2002;37:70–76.
  18. Bar-Shalom R, Yefremov N, Guralnik L, et al. Clinical performance of PET/CT in evaluation of cancer: additional value for diagnostic imaging and patient management. *J Nucl Med.* 2003;44:1200–1209.
  19. Turlakow A, Yeung HW, Pui J, et al. Fluorodeoxyglucose positron emission tomography in the diagnosis of giant cell arteritis. *Arch Intern Med.* 2001;161:1003–1007.
  20. Belhocine T, Blockmans D, Hustinx R, Vandevivere J, Mortelmans L. Imaging of large vessel vasculitis with  $^{18}\text{F}$ FDG PET: illusion or reality? A critical review of the literature data. *Eur J Nucl Med Mol Imaging.* 2003;30:1305–1313.
  21. Vallabhajosula S, Machac J, Knesaurek K, et al. Imaging atherosclerotic macrophage density by positron emission tomography using F-18-fluorodeoxyglucose (FDG) [abstract]. *J Nucl Med.* 1996;37(suppl):38P.
  22. Vallabhajosula S, Fuster V. Atherosclerosis: imaging techniques and the evolving role of nuclear medicine. *J Nucl Med.* 1997;38:1788–1796.
  23. Leeuw de K, Bijl M, Jager PL. Value of FDG PET in diagnosis and follow-up of patients with Takayasu arteritis [abstract]. *J Nucl Med.* 2003;44(suppl):46P.
  24. Tatsumi M, Cohade C, Nakamoto Y, Wahl RL. Fluorodeoxyglucose uptake in the aortic wall at PET/CT: possible finding for active atherosclerosis. *Radiology.* 2003;229:831–837.
  25. Hanif MZ, Ghesani M, Shah AA, Kasai T. F-18 Fluorodeoxyglucose uptake in atherosclerotic plaque in the mediastinum mimicking malignancy: another potential for error. *Clin Nucl Med.* 2004;29:93–95.

